Celebrating the Megascale: Proceedings of the Extraction and Processing Division Symposium on Pyrometallurgy in Honor of David G.C. Robertson
Edited by: Phillip J. Mackey, Eric J. Grimsey, Rodney T. Jones, and Geoffrey A. Brooks
TMS (The Minerals, Metals & Materials Society), 2014

MODELING OF LADLE METALLURGY IN STEELMAKING

Gordon Irons[1], Krishnakumar Krishnapisharody[2] and Kevin Graham[3]

[1]Steel Research Centre, McMaster University, Hamilton, Canada
[2]Saarstahl Innovation, Volklingen, Germany
[3]Strategic & Business Planning, Vale, Toronto, Canada

Keywords: Modeling, steelmaking, ladle metallurgy, injection, slag, reactions

Abstract

Ladle or secondary metallurgy in steelmaking is an essential process step for the production of high-quality steel. Professor David Robertson was a pioneer in the modeling of these processes, in particular gas-metal fluid dynamic interactions and the rates of slag-metal reactions. This is now a highly active area of research, and some of the recent developments in this area will be reviewed.

Introduction

Ladle or secondary steelmaking is the process step after primary steelmaking (BOF or EAF steelmaking) and before casting, so it is the final opportunity to modify the steel chemistry. Therefore, it is essential that the chemistry in terms of dissolved elements, and inclusion chemistry and size distribution be correct.

Gas injection is central to most Ladle Metallurgy operations. During ladle processing, the steel melt is usually stirred by an inert gas like Argon through porous plug(s) fitted in the bottom of the ladle or a lance inserted deep into the melt. The purging serves several purposes *viz.,* homogenizing the melt, flotation of inclusions, enhancing the rates both of refining reactions and dissolution of alloying elements and promoting inter-phase interactions in the ladle.

The other central issue to Ladle Metallurgy is the refining reactions between the synthetic top slag and the steel. Sulphur removal from the steel is the usual purpose of refining, but because this reaction is electrochemical coupled, other elements are affected. More recently, steelmakers have recognized that there is a direct link between the slag refining conditions and the inclusion composition.

Professor Robertson has made important contributions to both the areas of gas injection and refining reactions. Recent work following from his work in the authors' group will be briefly reviewed.

Gas Injection

Gas injection is widely used in metallurgical operations, and has been studied extensively. Figure 1a is taken from the work of Farias and Robertson [1]. In this work they injected different gases to investigate the effect of the gas to liquid density ratio on the gas behavior; at high jet momentum this is an important parameter. In Ladle Metallurgy, the flow rates are much lower, so the gas plume appears to be more like the water model in Figure 1b, taken from the work of Anagbo and Brimacombe [2].

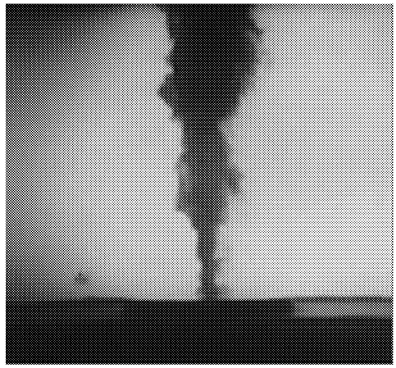

Figure 1(a). Nitrogen injection into water at high modified Froude number (Fr_m = 41000, d_o = 3.18 mm, Q = 8.3 x 10^{-3} m^3 s^{-1}, Farias and Robertson [1])

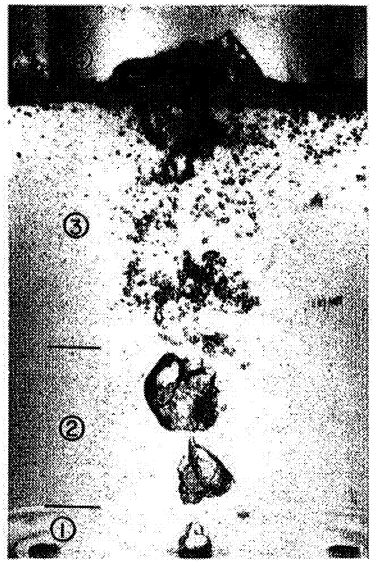

Figure 1(b). Air injection into water at low modified Froude number (Fr_m = 8, d_o = 6.35 mm, Q = 6.5 x 10^{-4} m^3 s^{-1}): the regimes of gas dispersion in liquid at low modified Froude numbers (1) Primary bubble (2) free bubble (3) plume and (4) spout, as represented by Anagbo *et al.* [2].

In a previous work by the present authors on the dynamics of two-phase plumes, [3] it was proven that only two dimensionless quantities are required to characterize free-rising plumes as in ladle metallurgy applications. These are the non-dimensionalized gas flow rate (Q^*) and axial height (z^*), defined, respectively, as:

$$Q^* = \frac{Q}{g^{0.5} H^{2.5}} \tag{1}$$

$$z^* = \frac{z}{H} \tag{2}$$

where Q is the gas flow rate, H is the metal height, z is the vertical position and g is the gravitational acceleration. It was also proven that the proper form of the Froude number relevant to Ladle Metallurgy is the plume Froude number, based on the liquid or plume velocity as the relevant velocity and the bath height as the characteristic dimension:

$$Fr_p = \frac{\overline{U}_l^2}{\overline{\alpha} g H} \tag{3}$$

The plume Froude number arose from the non-dimensionalization of the equation for momentum in the free-rising part of the plume. In that study the plume Froude number was mathematically related to Q^* [3]:

$$Fr_p = \Phi\left(Q^*, z^*\right) \tag{4}$$

Therefore, dynamic similarity is achieved by matching either Fr_p or Q^* and z^* in the plume. It is more convenient to use Q^* because it contains variables that are set by the operator.

Further, by using the mathematical descriptions of two-phase systems, *viz.*, (1) the well-known Eulerian-Lagrangian or bubble tracking models and (2) momentum and continuity for the phases, a similarity framework was developed to correlate all the major plume parameters to Q^* and z^* on a fundamental basis [3]. In this framework, the similarity parameters for the void fraction, plume radius, liquid and gas velocities, respectively are:

$$\overline{\alpha} = 1.13\left(Q^*\right)^{0.63}\left(z^*\right)^{-1.57} \tag{5}$$

$$R_p^* = \frac{R_p}{H} = 0.65\left(Q^*\right)^{0.2}\left(z^*\right)^{0.5} \tag{6}$$

$$\overline{U}_l^* = \frac{\overline{U}_l}{\sqrt{gH}} = 1.16\left(Q^*\right)^{0.32}\left(z^*\right)^{-0.28} \tag{7}$$

$$\overline{U}_g^* = \frac{\overline{U}_g}{\sqrt{gH}} = 3.52\left(Q^*\right)^{0.37}\left(z^*\right)^{-0.43} \tag{8}$$

where the overbar indicates that the quantity is averaged over the plume cross-section and the superscript * indicates that that the variable is non-dimensional.

The model was also extended to mixing times, t_m (the time to achieve a particular degree of chemical homogeneity, 95% in this case) as a function of gas injection rate [4]:

$$t_m^* = t_m\sqrt{\frac{g}{H}} = 82.4\ \left(Q^*\right)^{-0.31}\left(R^*\right)^2 \tag{9}$$

Where R^* is the dimensionless vessel radius:

$$R^* = \frac{R}{H} \tag{10}$$

The equations in this model, Equations 5 to 9, have been compared with all available data in Figure 2. Further details are contained in references [4] and [5]. It is clear that there is remarkably good agreement between the model and data over a wide range of conditions. It should also be noted that the model is entirely self-consistent which means that the variables scale properly, according to plume Froude number similarity. Those references [4, 5] further argue that because the *modified* Froude number (widely used in gas injection studies) and the specific energy input should not be used in ladle metallurgy applications because they do not conform to plume Froude number similarity.

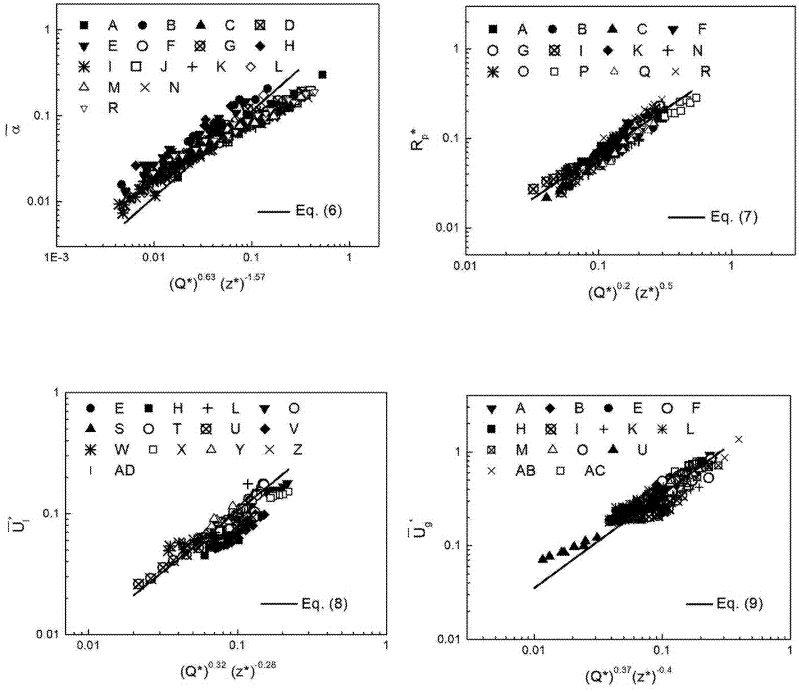

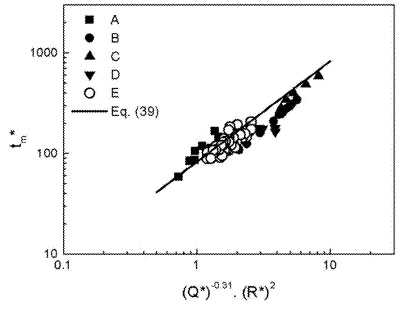

Figure 2: Similarity representation of the plume void fraction (a), plume radius (b), liquid velocity (c), gas velocity (d) and mixing time (e). The letters in the figures refer to the source of the data, explained in the original references [4, 5]. Equation 39 in Figure 2e is Equation 9 in this text.

Slag-Metal Reactions

It has been known since the work of King and Ramachandran [6] that slag-metal reactions are electrochemically coupled, but it has been difficult to develop a process model for Ladle Metallurgy reactions. The work of Robertson, Deo and Ohguchi [7] was a breakthrough in this regard, and it has been adopted by the present authors for a model of slag metal reactions in a full-scale Ladle Metallurgy station at ArcelorMittal Dofasco [8, 9]. The model is currently being extended to the transformation of inclusions.

The mixed mass transfer control model of Robertson *et al.* [7] is based on diffusion-controlled reactions in slag and metal, assuming equilibrium at the slag-metal interface. The generalized interfacial slag-metal reaction is:

$$x\underline{M} + y\underline{O} = M_xO_y \tag{11}$$

For which the equilibrium constant can be given as:

$$K_M = \frac{a_{M_xO_y}}{h_M^{\,x} h_O^{\,y}} \tag{12}$$

where K_m is the deoxidation constant, a_{MxOy} the activity of the interfacial oxide component, and h_O and h_M the respective interfacial Henrian activities for oxygen and selective metallic components in steel.

Assuming conservation of mass, flux density equations for each interfacial slag-metal reaction can be stated as:

$$k_m^M \, C_{Vm} \left(X_M^b - X_M^* \right) = k_{sl}^{M_xO_y} \, C_{Vs} \left(X_{M_xO_y}^* - X_{M_xO_y}^b \right) \tag{13}$$

where k_m^M and k_{sl}^{MxOy} are the mass transfer coefficients in the metal and slag phases for the

respective metal and oxide components, C_{Vm} and C_{Vs} represent the molar volumes of metal and slag, and X^b and X^* the bulk and interfacial mole fractions of metal and oxide components in either the slag and metal phases.

The basic approach proposed by Robertson et al. [7] involves first rearranging equation (12) for each slag-metal equilibrium reaction in terms of an expression for the interfacial oxide concentration. These derived expressions are then substituted into flux density equations (13) and manipulated in order to obtain relationships for the interfacial concentration of metallic components in terms of mass transfer coefficients and bulk metal and slag phase concentrations. Exact solution of the interfacial slag and metal concentration at any instant in time requires first coupling the various slag-metal reactions using an overall oxygen mass balance equation as:

$$k_m^O C_{Vm}\left(X_O^b - X_O^*\right) = \sum_{i=1}^{n} y_i C_{Vs}\, k_{sl}^{M_xO_y}\left(X_{M_xO_y}^* - X_{M_xO_y}^b\right) \tag{14}$$

Equation (14) expresses the fact that the total amount of oxygen change in the metal phase equals the total oxygen change in the slag phase. Substitution of the metallic and oxide interfacial concentration expressions into equation (14) yields a single non-linear equation containing only interfacial oxygen concentration as an unknown. A numerical solver based on the Newton-Raphson method was developed by the present authors for finding the root of the oxygen mass balance equation *(i.e.* the interfacial oxygen content). Having solved for the oxygen concentration at the interface, all other interfacial values can be determined and composition trajectories can be projected forward by numerical integration of first order differential equations of the form:

$$-\frac{dX_M}{dt} = k_m^M\left(\frac{A}{V_m}\right)\left(X_M^b - X_M^*\right) \tag{15}$$

$$\frac{dX_{M_xO_y}}{dt} = k_{sl}^{M_xO_y}\left(\frac{A}{V_{sl}}\right)\left(X_{M_xO_y}^* - X_{M_xO_y}^b\right) \tag{16}$$

The model was applied to results obtained at ArcelorMittal Dofasco. Figure 3 shows the way in which the gas flow rate through porous plugs, total electrical power input and alloy additions are made in a typical heat. No modifications were made to operating practice; the model inputs were made to change as they did in the plant.

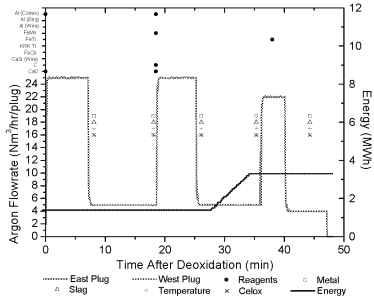

Figure 3: Summary of stirring, heating, alloy addition, and sampling procedure for one typical heat at ArcelorMittal Dofasco.

The model requires known values for the mass transfer coefficients. These were deduced from analysis of the rate of desulphurization. The rate was found to be dependent on the gas flow rate as shown in Figure 4.

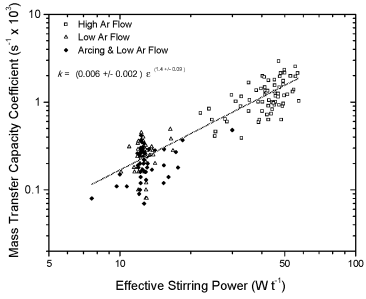

Figure 4: Relationship between mass transfer capacity coefficient for sulphur and effective stirring power which is proportional to the gas flow rate.

The results were validated against 41 heats at ArcelorMittal Dofasco. Figure 5 shows the agreement between the model and experiment for heat 40. At the 18 minute mark aluminum was added to the steel and the stirring rate was increased which lead to a rapid decrease in the sulphur content. These conditions were so reducing that silica and manganese oxide were reduced from the slag into the melt. As can be seen, these changes are well-described by the model.

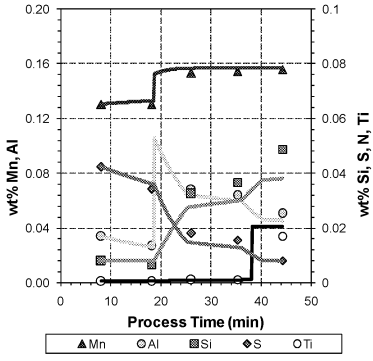

Figure 5a: Comparison of the model and experimental data for heat 40. At 18 minutes aluminum was added, and the gas stirring rate was increased. At 38 minutes titanium was added.

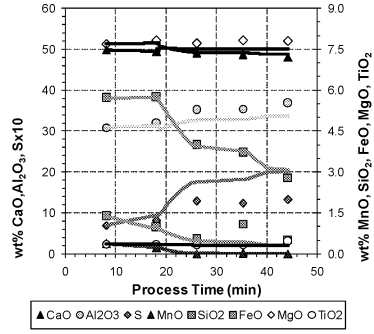

Figure 5 b: Comparison of slag compositions for the model and data for Heat 40.

Summary

The hallmark of Professor Robertson's work is that he has applied fundamental approaches to solving significant problems in metals processing. His works cited in this paper are just two examples of the many fine contributions that he has made. On a personal note, it has always been a pleasure to discuss our mutual interests, and he has been very gracious with my students as well.

References

1. L.R. Farias and D.G.C. Robertson, Private Communication, 1982.

2. P.E. Anagbo, J.K. Brimacombe and A.H. Castillejos, A Unified Representation of Gas Dispersion in Upwardly Injected Submerged Gas Jets, *Can. Metall. Q.*, 1989, 28, 323-30.

3. K. Krishnapisharody and G. A. Irons, "A Unified Approach to the Fluid Dynamics of Gas-Liquid Plumes in Ladle Metallurgy", *ISIJ International*, 50, (10), 1413-1421.

4. K. Krishnapisharody and G. A. Irons, "An Analysis of Recirculatory Flow in Gas-Stirred Ladles", *Materials Processing Towards Properties, Seetharaman Seminar*, June 14 - 15, 2010, Stockholm, Jernkontoret, 317 – 326.

5. K. Krishnapisharody and G.A. Irons, "A Critical Review of the Modified Froude Number in Ladle Metallurgy", in press, *Metallurgical and Materials Transactions B*, 2013.

6. S. Ramachandran, T.B. King, and N.J. Grant: Trans. AIME, 206 (1956) 1549-53.

7. D.G.C. Robertson, B. Deo, and S. Ohguchi, "A Multicomponent Mixed Transport Control Theory for the Kinetics of Coupled Slag/Metal and Slag/Metal/Gas Reactions: Application to Desulphurization of Molten Iron", *Ironmaking and Steelmaking*, 1984, 11, 41-55.

8. K.J. Graham and G.A. Irons, Towards Integrated Ladle Metallurgy Control, *Proceedings AISTech2008*, Pittsburgh, Pa, May 5-8, 2008, AIST, 13.

9. K.J. Graham and G.A. Irons, , Coupled Kinetic Phenomena in Ladle Metallurgy, *International Symposium on Highly Innovative Novel Operations "Future Steelmaking Metallurgy"*, Tokyo, May 23-25, 2010, ISIJ and JSPS, 65 - 74.